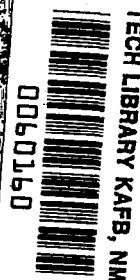
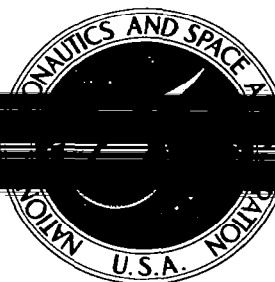


NASA CR-845



A METHOD OF CALCULATING WIND TUNNEL INTERFERENCE FACTORS FOR TUNNELS OF ARBITRARY CROSS-SECTION

by Robert G. Joppa

Prepared by
UNIVERSITY OF WASHINGTON
Seattle, Wash.
for

NATIONAL AERONAUTICS AND SPACE ADMINISTRATION • WASHINGTON, D. C. • JULY 1967



A METHOD OF CALCULATING
WIND TUNNEL INTERFERENCE FACTORS
FOR TUNNELS OF ARBITRARY CROSS-SECTION

By Robert G. Joppa

Distribution of this report is provided in the interest of information exchange. Responsibility for the contents resides in the author or organization that prepared it.

Prepared under Grant No. NGR-48-002-010 by
COLLEGE OF ENGINEERING
UNIVERSITY OF WASHINGTON
Seattle, Wash.

for

NATIONAL AERONAUTICS AND SPACE ADMINISTRATION

A METHOD OF CALCULATING
WIND TUNNEL INTERFERENCE FACTORS
FOR TUNNELS OF ARBITRARY CROSS-SECTION

By Robert G. Joppa

SUMMARY

A new method of calculating the wind tunnel wall induced interference factors has been developed. The tunnel walls are represented by a vortex lattice of strength sufficient to satisfy the boundary conditions at the wall. The vortex lattice is then used to calculate the interference velocities at any point in the wind tunnel. The resulting interference factors agree with the classical results that are available for square and circular tunnels. Calculations are also presented for a rectangular tunnel, and they can be made to closely approximate a tunnel of any cross-section.

INTRODUCTION

Current interest in V/STOL aircraft has resulted in a renewed interest in the problems of the wind tunnel measurement of their characteristics. Among the problems of critical importance is that of calculating the interference velocities due to the presence of the tunnel walls, particularly the longitudinal distribution of the

interference because of its large effect on the measured pitching moment. Classical methods of computing these interference velocities are inadequate for V/STOL models that characteristically produce large downwash, and so a new method is required to handle this case. In this report a new method of representing the tunnel walls is developed which should be applicable to the large downwash case, and it is tested by being applied to the limiting case of small downwash in order to compare results with classical theory.

The classical solutions have depended upon the assumption of a proper set of images outside the tunnel, of the vortex flow inside the tunnel, such that the walls become streamlines. Unfortunately, no proper image system has been found for any tunnel except the rectangular cross-sections. Prandtl (Ref. 1) has presented a solution for the circular wind tunnel with an undeflected wake which gives correct values of upwash at the wing. Glauert (Ref. 2) has solved the rectangular wind tunnel problem, including the effects downstream, i.e., at the tail location. Others (Refs. 3 to 9) have extended it to include other tunnel shapes. Lotz (Ref. 10) has offered a solution for the upwash interference for circular and elliptical tunnels which will yield results at downstream locations as well as at the wing. In Lotz's solution, an image system is used which is valid at the wing and far downstream, and an additional potential function is assumed in infinite series form which is required to cancel the remaining normal velocities

at the wall, also expressed in series form. To the degree that these series do not completely converge before being truncated, this solution is an approximation.

The object of this work is to present an alternate method of representing the tunnel walls which would be applicable to a tunnel of any arbitrary cross-section and which could be extended to handle the large downwash case. It is hypothesized that the tunnel walls might be represented by a network of vortex lines whose magnitude and direction are just sufficient to prevent flow through a set of control points on the walls. The approach is similar to that of approximate lifting surface theory.

This paper presents the mathematical development of the theory. The results of sample calculations for the interference factors and the distribution of interference over the longitudinal and lateral axes are presented for uniformly loaded wings of various spans in a variety of wind tunnels. The wind tunnel configurations include square, rectangular and circular cross-sections. These results are then compared, where possible, with prior work which have obtained corresponding values by other theoretical treatments.

SYMBOLS

b	Wing vortex span
c	Wind tunnel cross-section area
C_L	Wing lift coefficient

$h()$	Normal distance to a point p from a line containing a vortex segment identified by subscript
$h()()$	Normal distance to a point p from a plane containing vortex segments identified by subscript
H	Height of wind tunnel
$\bar{i}, \bar{j}, \bar{k}$	Unit vectors in the directions X, Y, Z
L, G	Dimensions of rectangular vortex ring (Fig. 3)
\bar{n}	Unit vector normal to vortex ring
$R()$	Vector from point (X,Y,Z) to end of a vortex vector \bar{S} indicated by subscript
$R()()$	Magnitude of component of vector $R()$ indicated by second subscript
s	Wing area
\bar{S}	Vector representing a vortex segment of strength Γ and length S
$S()$	Component of \bar{S} indicated by subscript
\bar{v}	Unit vector in the direction of the total velocity vector at a point
\bar{V}	Velocity induced at a point
w	Vertical component of wall-induced interference velocity
W	Width of wind tunnel
\bar{W}	Vector representing a wing bound vortex of strength Γ_w
X,Y,Z	Cartesian coordinate of a point (see Fig. 1)
β	Angles defining direction to a point from the end of a vortex segment (Fig. 2)
Γ	Circulation strength of a vortex
δ	Tunnel-wall-induced interference factor

STATEMENT OF PROBLEM

The problem is to find that distribution of vorticity lying in the tunnel walls which will prevent any flow through the wall due to the action of a lifting system in the wind tunnel. The lifting surface is assumed to be uniformly loaded and is represented by a simple horseshoe vortex with the trailing pair undeflected. In principle, any desired distribution of lift could be built up of such simple elements.

The walls are represented by a tubular vortex sheet of finite length composed of a network of circumferential and longitudinal vortices having equal spacing (Fig. 1). Helmholtz' theorem that a vortex filament can neither end nor begin in the flow is satisfied most readily by constructing the network of square vortex rings lying wholly within the plane of the walls. Each such square has a vortex strength Γ_i , and each side is coincident with the side of the neighboring square. Thus, the strength of any segment is the sum of the strengths of the two adjoining squares. The boundary condition that the wall must be impervious to flow is satisfied at a control point in the center of each square. This results in a set of simultaneous equations, one written for each control point, in which the unknowns are the Γ_i .

A large number of equations results if the tube is very long, thus some judgment is required in choosing the geometric arrangement. The use of square vortex rings requires a tunnel of constant cross-section. One notes that for a wing mounted in the center

of the tunnel, lateral symmetry always exists; and if the wake is undeflected, vertical symmetry also exists, thus reducing the number of unknowns. The trailing edge of the finite length tube which represents the long tunnel requires a slightly different treatment. At a far downstream section only longitudinal vorticity should exist. This is represented by elongating the last ring of squares by a large amount, while keeping the control point at the same location with respect to the last circumferential station. Figure 1 shows the arrangement for a rectangular tunnel with filleted corners.

SETUP OF THE EQUATIONS

A right-hand axis system is established with the X-axis on the longitudinal centerline of the tunnel, positive downstream. The Y-axis is taken positive upward and the Z-axis positive to the right side of the tube facing downstream.

Since the surface of the tunnel is to be made of square elements, its cross-section is a polygon of equal segments arranged to approximate any desired shape. In this development the cross-section will be assumed to be symmetrical about the X,Y plane.

In general, the velocity induced at any point p (Fig. 2) due to a vortex segment may be written:

$$\bar{V} = \frac{\Gamma}{4\pi h} (\cos \beta_1 + \cos \beta_2) \bar{v} \quad (1)$$

The terms required are written as follows:

$$\cos \beta_1 + \cos \beta_2 = \frac{R_1 + R_2}{2R_1 R_2 S} \left[S^2 - (R_1 - R_2)^2 \right]$$

$$\bar{v} = \frac{\bar{R}_1 \times \bar{S}}{|\bar{R}_1 \times \bar{S}|} = \frac{\begin{vmatrix} \bar{i} & \bar{j} & \bar{k} \\ R_{1x} & R_{1y} & R_{1z} \\ S_x & S_y & S_z \end{vmatrix}}{R_1 S \sin \beta_1}$$

$$\text{But } \sin \beta_1 = \frac{h}{R_1}$$

$$\bar{v} = \frac{\begin{pmatrix} R_{1y} S_z - R_{1z} S_y \end{pmatrix} \bar{i}}{Sh} - \frac{\begin{pmatrix} R_{1x} S_z - R_{1z} S_x \end{pmatrix} \bar{j}}{Sh} + \frac{\begin{pmatrix} R_{1x} S_y - R_{1y} S_x \end{pmatrix} \bar{k}}{Sh}$$

Finally, the velocity induced at a point due to a vortex segment is:

$$\frac{\bar{v}}{\Gamma/4\pi h} = \frac{R_1 + R_2}{2R_1 R_2 S^2 h} \left[S^2 - (R_1 - R_2)^2 \right] \left[\begin{pmatrix} R_{1y} S_z - R_{1z} S_y \end{pmatrix} \bar{i} \right. \\ \left. + \begin{pmatrix} R_{1z} S_x - R_{1x} S_z \end{pmatrix} \bar{j} + \begin{pmatrix} R_{1x} S_y - R_{1y} S_x \end{pmatrix} \bar{k} \right] \quad (2)$$

One could then add the contributions of all four sides of a vortex square, but it is more convenient to take advantage of the lateral symmetry and sum the effects due to a pair of symmetrically located vortex squares of the same strength. The arrangement is shown in Figure 3 and the following equation results:

$$\frac{\bar{V}}{\Gamma/8\pi L} = h_{AB} \left\{ \frac{\frac{R_{NA}+R_{NB}}{2}}{h_{N_1}^2 R_{NA} R_{NB}} \left[L^2 - (R_{NA}-R_{NB})^2 \right] - \frac{\frac{R_{MA}+R_{MB}}{2}}{h_{M_1}^2 R_{MA} R_{MB}} \left[L^2 - (R_{MA}-R_{MB})^2 \right] \right\} \bar{i}$$

$$+ h_{DC} \left\{ \frac{\frac{R_{ND}+R_{NC}}{2}}{h_{N_2}^2 R_{ND} R_{NC}} \left[L^2 - (R_{ND}-R_{NC})^2 \right] - \frac{\frac{R_{MD}+R_{MC}}{2}}{h_{M_2}^2 R_{MD} R_{MC}} \left[L^2 - (R_{MD}-R_{MC})^2 \right] \right\} \bar{i} \quad (3)$$

$$+ \cos \phi_B \left\{ \frac{\frac{R_{NA}+R_{NB}}{2}}{h_{N_1}^2 R_{NA} R_{NB}} \left[L^2 - (R_{NA}-R_{NB})^2 \right] + \frac{\frac{R_{ND}+R_{NC}}{2}}{h_{N_2}^2 R_{ND} R_{NC}} \left[L^2 - (R_{ND}-R_{NC})^2 \right] \right\} (X_N - X) \bar{j}$$

$$+ \cos \phi_B \left\{ \frac{\frac{R_{MA}+R_{MB}}{2}}{h_{M_1}^2 R_{MA} R_{MB}} \left[L^2 - (R_{MA}-R_{MB})^2 \right] + \frac{\frac{R_{MD}+R_{MC}}{2}}{h_{M_2}^2 R_{MD} R_{MC}} \left[L^2 - (R_{MC}-R_{MB})^2 \right] \right\} (X_M - X) \bar{j}$$

6

$$\begin{aligned}
 & + \left\{ \frac{R_{MA} + R_{NA}}{h_A^2 R_{MA} R_{NA}} \left[L^2 - (R_{MA} - R_{NA})^2 \right] (Z - Z_A) + \frac{R_{NB} + R_{MB}}{h_B^2 R_{NB} R_{MB}} \left[L^2 - (R_{MB} - R_{NB})^2 \right] (Z_B - Z) \right\} \bar{j} \\
 & + \left\{ \frac{R_{NC} + R_{MC}}{h_C^2 R_{NC} R_{MC}} \left[L^2 - (R_{NC} - R_{MC})^2 \right] (Z_C - Z) + \frac{R_{ND} + R_{MD}}{h_D^2 R_{ND} R_{MD}} \left[L^2 - (R_{ND} - R_{MD})^2 \right] (Z - Z_D) \right\} \bar{j} \\
 & + \sin \phi_B \left\{ \frac{R_{NA} + R_{NB}}{h_{N1}^2 R_{NA} R_{NB}} \left[L^2 - (R_{NA} - R_{NB})^2 \right] - \frac{R_{NC} + R_{ND}}{h_{N2}^2 R_{NC} R_{ND}} \left[L^2 - (R_{NC} - R_{ND})^2 \right] \right\} (X_N - X) \bar{k} \\
 & + \sin \phi_B \left\{ \frac{R_{MC} + R_{MD}}{h_{M2}^2 R_{MC} R_{MD}} \left[L^2 - (R_{MC} - R_{MD})^2 \right] - \frac{R_{MA} + R_{MB}}{h_{M1}^2 R_{MA} R_{MB}} \left[L^2 - (R_{MA} - R_{MB})^2 \right] \right\} (X_M - X) \bar{k} \\
 & + \left\{ \frac{R_{NA} + R_{MA}}{h_A^2 R_{NA} R_{MA}} \left[L^2 - (R_{NA} - R_{MA})^2 \right] - \frac{R_{NC} + R_{MC}}{h_C^2 R_{NC} R_{MC}} \left[L^2 - (R_{NC} - R_{MC})^2 \right] \right\} (Y_A - Y) \bar{k} \\
 & + \left\{ \frac{R_{ND} + R_{MD}}{h_D^2 R_{ND} R_{MD}} \left[L^2 - (R_{ND} - R_{MD})^2 \right] - \frac{R_{NB} + R_{MB}}{h_B^2 R_{NB} R_{MB}} \left[L^2 - (R_{NB} - R_{MB})^2 \right] \right\} (Y_B - Y) \bar{k}
 \end{aligned}$$

Similarly, the velocity induced at point p by a simple horse-shoe vortex located in the center of the tunnel is derived from Figure 4 using eq. (1). Summing the contributions from the three segments yields:

$$\begin{aligned} \frac{\bar{V}}{\Gamma_w/8\pi b} = & - \frac{R_{W1}+R_{W2}}{h_b^2 R_{W1}R_{W2}} \left[b^2 - (R_{W1}-R_{W2})^2 \right] R_{W1_y} \bar{i} \quad (4) \\ & + \left\{ \frac{2b}{h_2^2} \left(1 + \frac{X-X_w}{R_{W2}} \right) R_{W2_z} - \frac{2b}{h_1^2} \left(1 + \frac{X-X_w}{R_{W1}} \right) R_{W1_z} \right. \\ & \quad \left. + \frac{R_{W1}+R_{W2}}{h_b^2 R_{W1}R_{W2}} \left[b^2 - (R_{W1}-R_{W2})^2 \right] R_{W1_x} \right\} \bar{j} \\ & + \left\{ \frac{2b}{h_1^2} \left(1 + \frac{X-X_w}{R_{W1}} \right) R_{W1_y} - \frac{2b}{h_2^2} \left(1 + \frac{X-X_w}{R_{W2}} \right) R_{W2_y} \right\} \bar{k} \end{aligned}$$

The boundary condition is expressed at each control point by writing $\bar{V} \cdot \bar{n} = 0$ where \bar{n} is the unit outer normal to the surface at that point.

$$\bar{n} = \frac{\bar{i} \times (\bar{R}_1 - \bar{R}_2)}{|\bar{i} \times (\bar{R}_1 - \bar{R}_2)|}$$

Thus there is a set of N equations, one for each control point. Because of the right and left symmetry and vertical symmetry, there are $N/4$ unknown Γ_i . An electronic computer is used to solve the matrix for the Γ_i .

Once the Γ_i are known, the induced velocity due to the walls can be calculated at any point in the tunnel by the use of eq. (3) summed over all the vortex rings in the tunnel walls. The interference is expressed as an angle whose tangent is the vertical component of interference velocity divided by the tunnel wind speed. Results are expressed in terms of the classical interference factor δ , defined by the equation:

$$\Delta\alpha = \delta \frac{S}{c} C_L$$

The factor is computed in terms of wing circulation and vortex span

$$\delta = \frac{w c}{2b \Gamma_w}$$

Results are presented graphically to show the longitudinal variation of the factor δ for different wing spans in a variety of tunnels.

RESULTS OF CALCULATIONS

Results of calculations made for three representative tunnel shapes are presented in the form of graphs of the wall interference factor δ . Values of δ were calculated at points along the tunnel centerline from the wing location downstream for several values of wing vortex span. These are presented for a circular, a square, and a 3:5 rectangular tunnel in Figures 5, 6, and 7. The average value of this interference factor over the vortex span of the uniformly loaded wing was also calculated and is shown as a function of vortex span for each of these tunnels along with the centerline values in Figure 8.

COMPARISON OF RESULTS WITH CLASSICAL WORK

Square Tunnel

Very little previous work exists which can be used for a check on the accuracy or convergence of the present method. Prandtl's concept of an infinite array of images of the wing located outside the tunnel is applicable only to rectangular (including square) tunnels and has been applied by Silverstein & White in Reference 9. Results are presented there for square and 2:1 rectangular tunnels; only the square tunnel results are used for comparison, since 2:1 tunnels are not common.

The number of line segments, each corresponding to the side of a vortex square, to be used to adequately represent the square

tunnel cross-section was determined by making a series of calculations with increasing numbers of segments. Figure 9 shows the results of using 12, 16, and 20 segments to make up the periphery of the square cross-section. The results for 16 and 20 segments differ only slightly and correspond very closely to the data taken from Reference 9. The excellent agreement shown indicates that 16 segments are enough to represent satisfactorily the square cross-section tunnel.

Circular Tunnel

In the case of the circular tunnel, no exact solution is available for the downstream interference factors, so two approximate results are compared with the new calculations in Figure 10. The treatment presented by Lotz (Ref. 10) would be exact except that the numerical values depend upon the point at which an infinite series is truncated. Reference 10 gives no indication of the accuracy expected in its numerical values. The result taken from Silverstein & White (Ref. 9) was arrived at by following their suggestion that the downstream interference factors for the circular tunnel be taken as the same as for the square tunnel of the same area.

Four different approximations to the circular tunnel were used for this calculation. Two regular polygons having 12 or 16 sides were used for the cross-section shape; each was rotated so that either points or flats of the polygon were at the top and side centerline. All four calculations yielded the same curve, with

values within one-tenth of one percent. Thus, it is concluded that a 12-sided polygon is adequate to represent the circular tunnel.

Length Effect

The effect of length of the tunnel to be used in calculations was explored for the circular tunnel. A twelve-sided polygon was used in the calculation, with the model vortex span equal to 0.4 of the tunnel diameter. It is evident from Figure 11 that a length-to-diameter ratio of 3 or 4 is ample for convergence. The reason for this may be seen in an examination of the distribution of the wall vorticity. The bound vortex of the wing requires some circumferential vorticity in the walls, but only in the region quite near to the wing. Longitudinal vorticity is not required far upstream, and far downstream only longitudinal filaments exist to control the trailing pair from the wing. By using the artifice of a very long last ring, the proper conditions are met far downstream, and the vortex lattice need only be long enough to provide the circumferential vorticity needed in the immediate vicinity of the wing. In fact, all the vorticity in the circumferential rings is quickly transferred to the longitudinal filaments.

Figure 12 shows the wall vortex strengths taken from calculations made for circular tunnels of various lengths. The circumferential vorticity strengths were taken at the floor near the center of the tunnel where they are the strongest; the longitudinal vortex filament strength is that along the side wall at model height. It is evident that the details of the distribution are not strongly

affected by the presence or absence of tunnel walls more than about one diameter up or downstream from the wing.

CONCLUSIONS

A new method of calculating the tunnel-induced interference velocities has been developed which depends on the representation of the walls by a network of square vortex rings.

The method may be used to represent any tunnel cross-section by using an equivalent polygon of equal length sides and having the same cross-section area.

The method yields interference factors that agree with classical theory where that is available.

REFERENCES

1. Prandtl, L.: Tragflugeltheorie. II C, Göttingen Nachrichten, 1919.
2. Glauert, H.: The Interference of Wind Channel Walls on the Aerodynamic Characteristics of an Aerofoil. R. & M. No. 867, British A. R. C., 1923.
3. Glauert, H.: The Interference on the Characteristics of an Aerofoil in a Wind Tunnel of Rectangular Section. R. & M. No. 1459, British A. R. C., 1932.
4. Terazawa, Kwan-ichi: On the Interference of Wind Tunnel Walls of Rectangular Cross-Section on the Aerodynamical Characteristics of a Wing. Report No. 44, Aero. Res. Inst., Tokyo Imperial University, 1928.
5. Theodorsen, Theodore: The Theory of Wind-Tunnel Wall Interference. T. R. No. 410, N.A.C.A., 1931.
6. Theodorsen, Theodore: Interference on an Airfoil of Finite Span in an Open Rectangular Wind Tunnel. T.R. No. 461, N.A.C.A., 1933.
7. Rosenhead, L.: The Effect of Wind Tunnel Interference on the Characteristics of an Aerofoil. Roy. Soc. Proc., Math. and Phys., 129A, (London), 1930, pp. 115-135.
8. Tani, Itiro, and Sanuki, Matao: The Wall Interference of a Wind Tunnel of Elliptic Cross Section. Proceedings of the Physics-Math. Soc. of Japan, 3d Series, Vol. 14, No. 10, 1932.
9. Silverstein, A., and White, J. A.: Wind-Tunnel Interference with Particular Reference to Off-Center Positions of the Wing and to the Downwash at the Tail. T.R. No. 547, N.A.C.A., 1935.

10. Lotz, Irmgard: Correction of Downwash in Wind Tunnels of Circular and Elliptic Section. T.M. No. 801, N.A.C.A., 1936.

FIGURES

1. Representation of a Rectangular Tunnel with Corner Fillets by a Vortex Lattice of Square Vortex Rings Lying in the Tunnel Walls.
2. Velocity Induced at a Point by an Arbitrarily Oriented Vortex Segment.
3. Definition of Angles and Distances for a Pair of Vortex Squares Oriented Symmetrically about the X, Y Plane.
4. Definition of Distances for a Horseshoe Vortex Representing a Wing Located with its Midspan at the Origin of Coordinates.
5. Wall Interference Factors for a Circular Wind Tunnel.
6. Wall Interference Factors for a Square Wind Tunnel.
7. Wall Interference Factors for a 3:5 Rectangular Wind Tunnel.
8. Effect of Wing Span on Average Interference Factor and the Centerline Interference Factor at the Wing.
9. Comparison of Interference Factors with Classical Values for a Square Tunnel.
10. Comparison of Interference Factors with Classical Values for a Circular Tunnel.
11. Effect of Tunnel Length on Interference Factors for a Circular Tunnel.
12. Effect of Tunnel Length on Wall Vorticity Distribution for a Circular Tunnel.

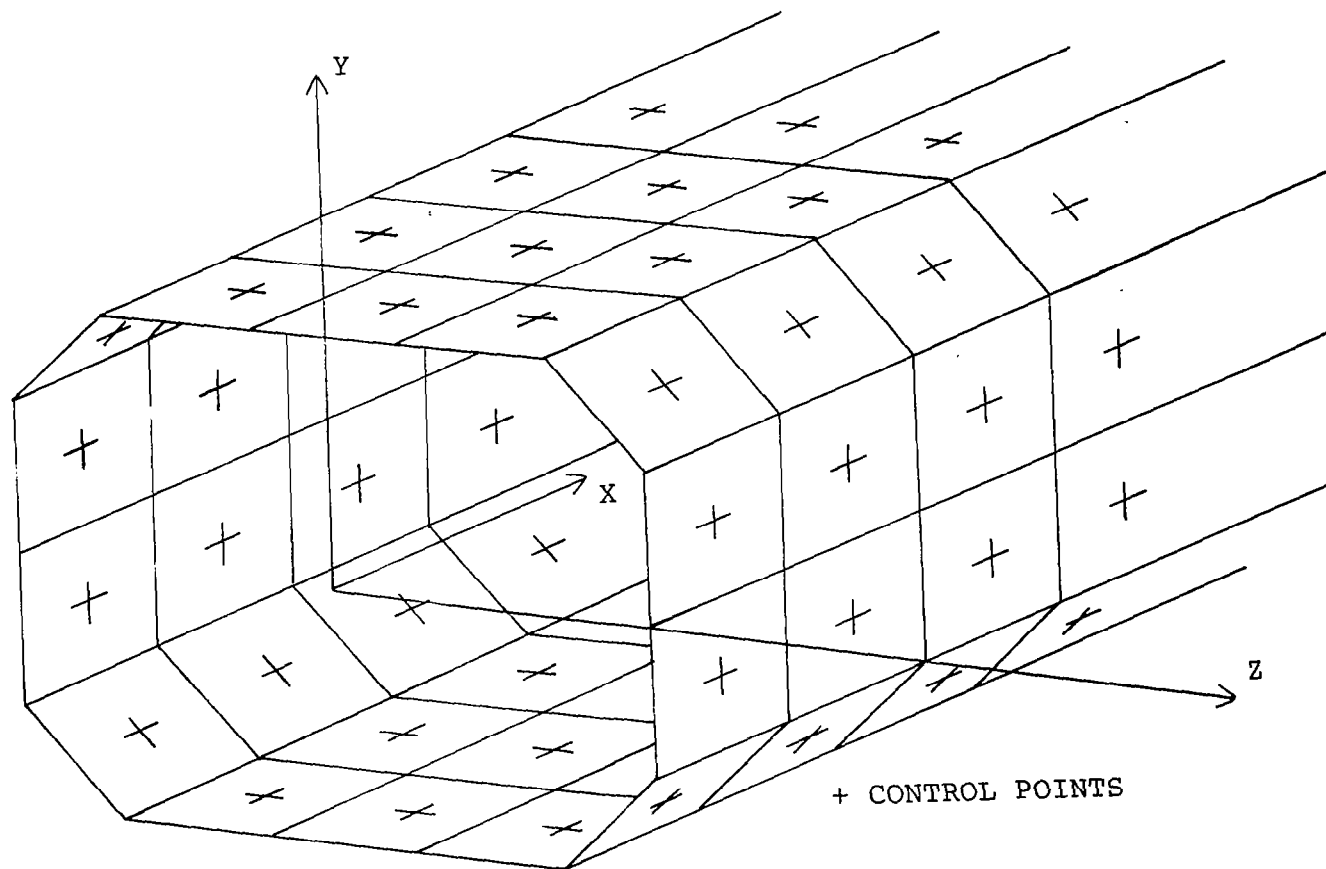


FIGURE 1
 REPRESENTATION OF A RECTANGULAR TUNNEL WITH CORNER FILLETS
 BY A VORTEX LATTICE OF SQUARE VORTEX RINGS LYING IN THE TUNNEL WALLS

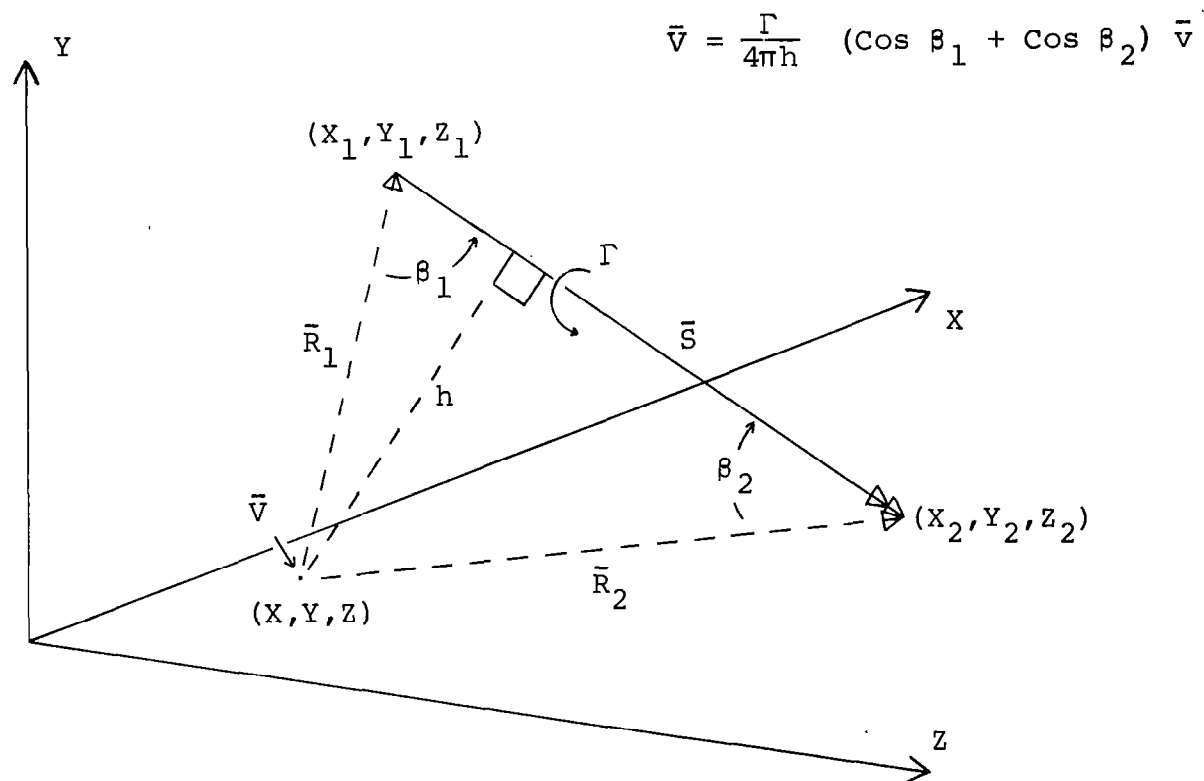


FIGURE 2

VELOCITY INDUCED AT A POINT BY AN ARBITRARILY ORIENTED VORTEX SEGMENT

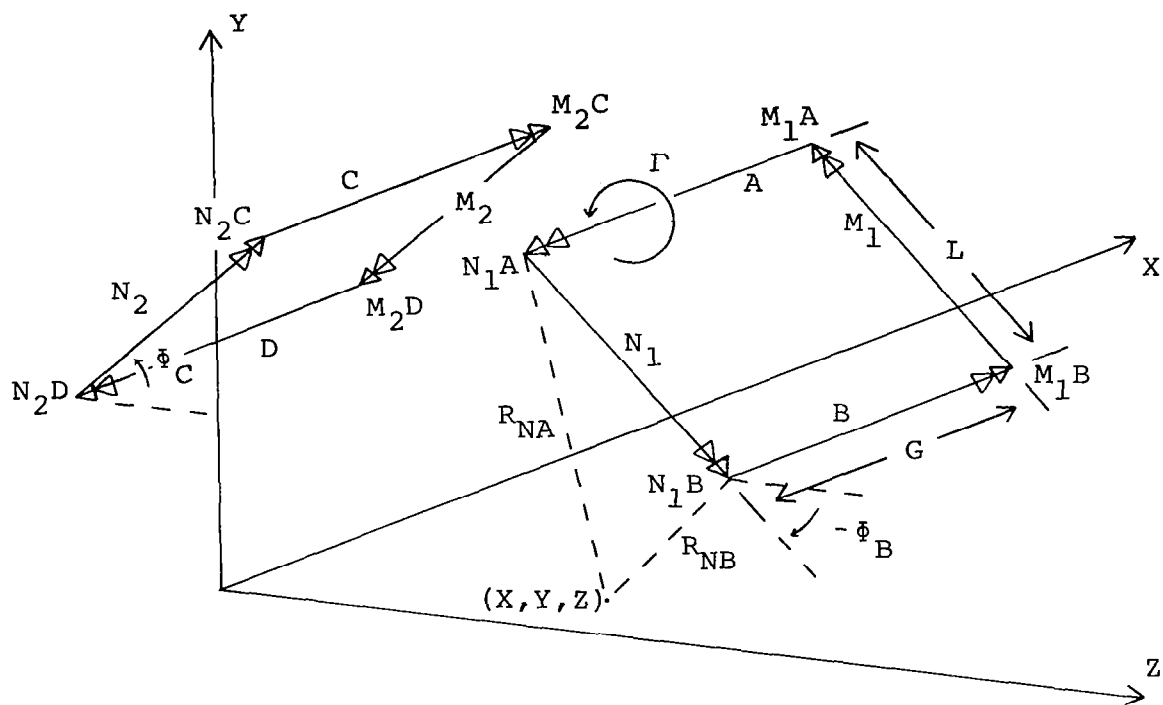


FIGURE 3

DEFINITION OF ANGLES AND DISTANCES FOR A PAIR OF VORTEX SQUARES
 ORIENTED SYMMETRICALLY ABOUT THE X,Y PLANE
 (ELEMENTS A, B, C, & D ARE PARALLEL TO THE X-AXIS)

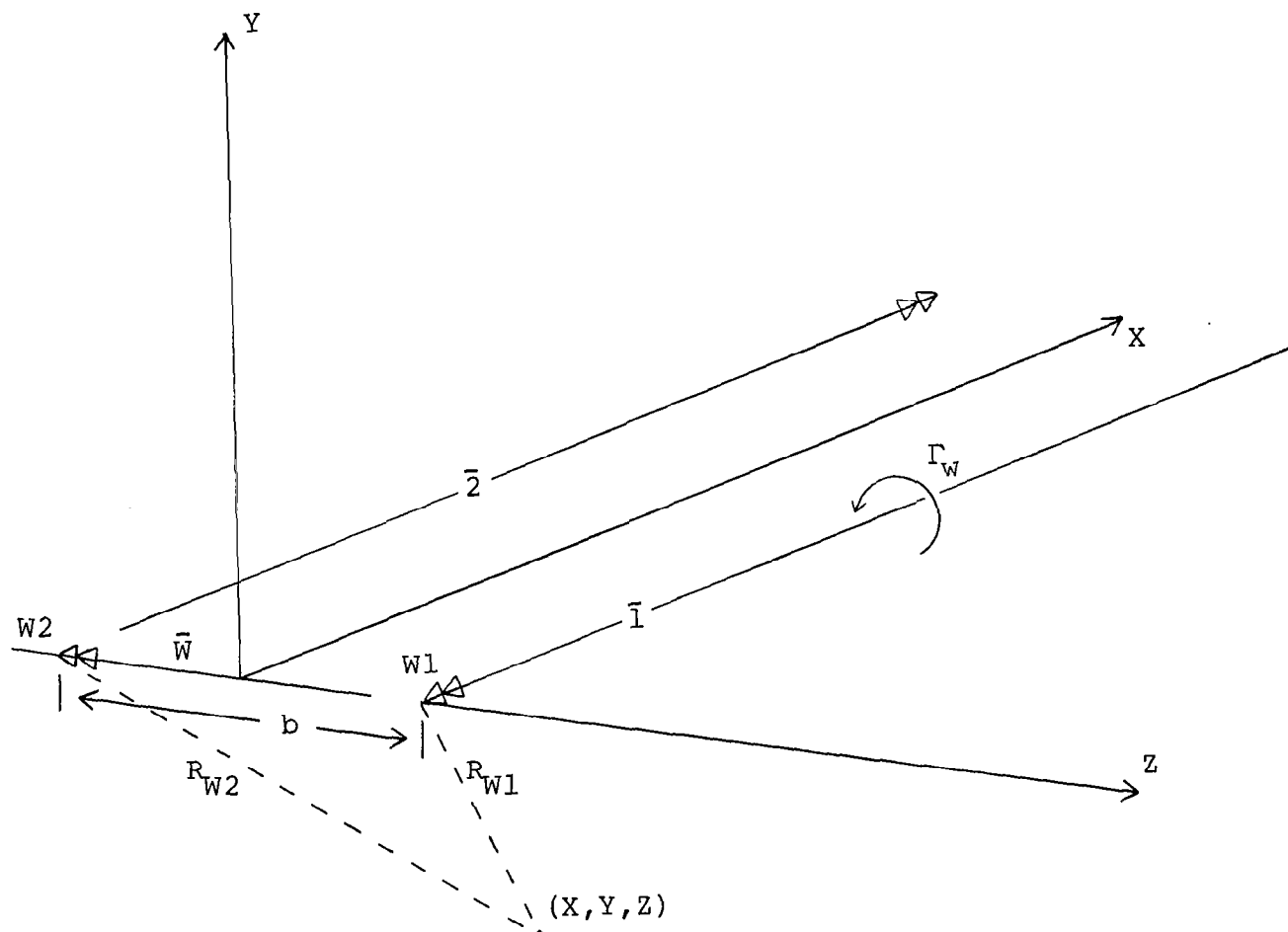


FIGURE 4

DEFINITION OF DISTANCES FOR A HORSESHOE VORTEX
 REPRESENTING A WING LOCATED WITH ITS MIDSPAN AT THE ORIGIN OF COORDINATES

WALL INTERFERENCE FACTORS
FOR A CIRCULAR WIND TUNNEL

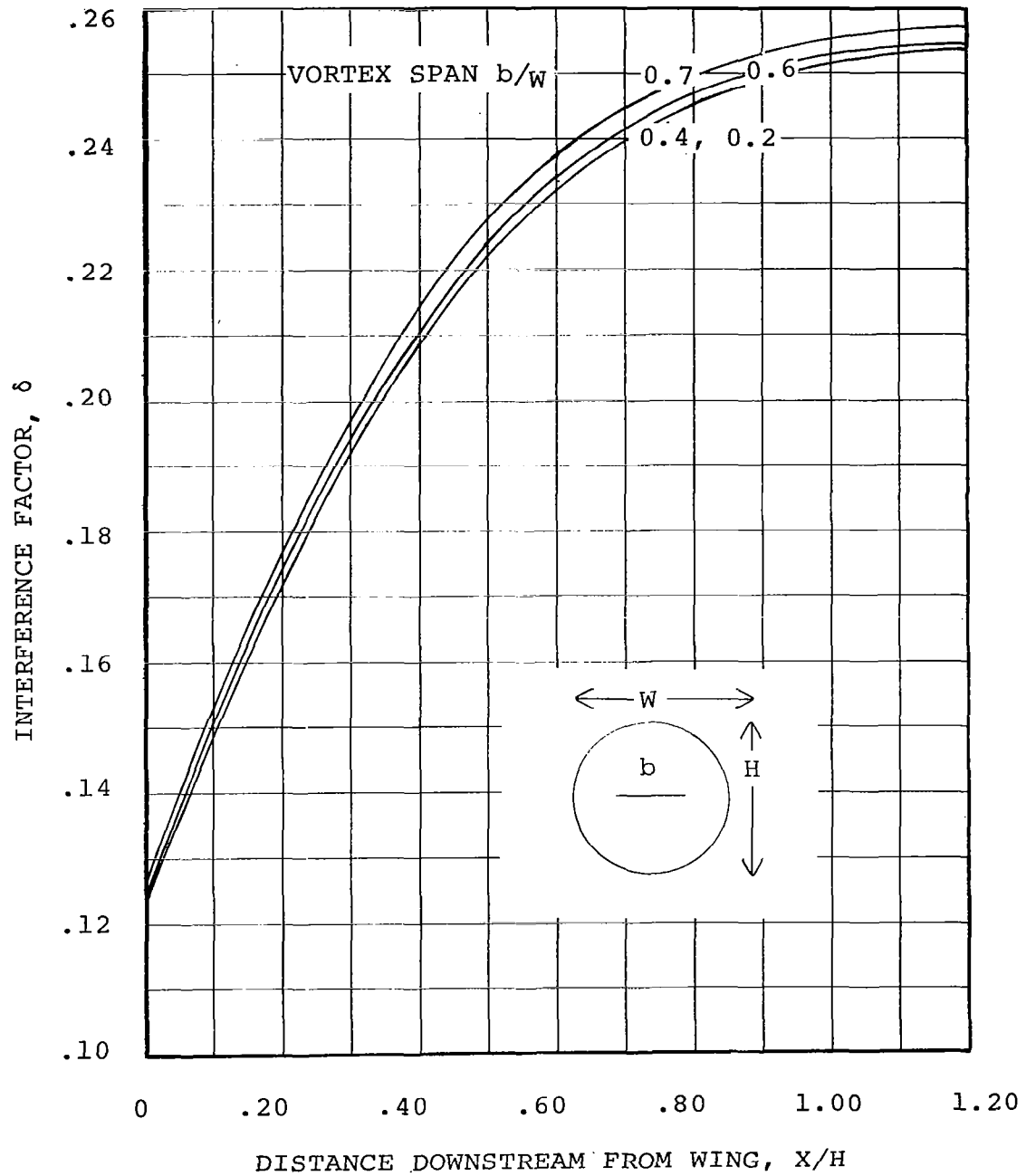


FIGURE 5

WALL INTERFERENCE FACTORS
FOR A SQUARE WIND TUNNEL

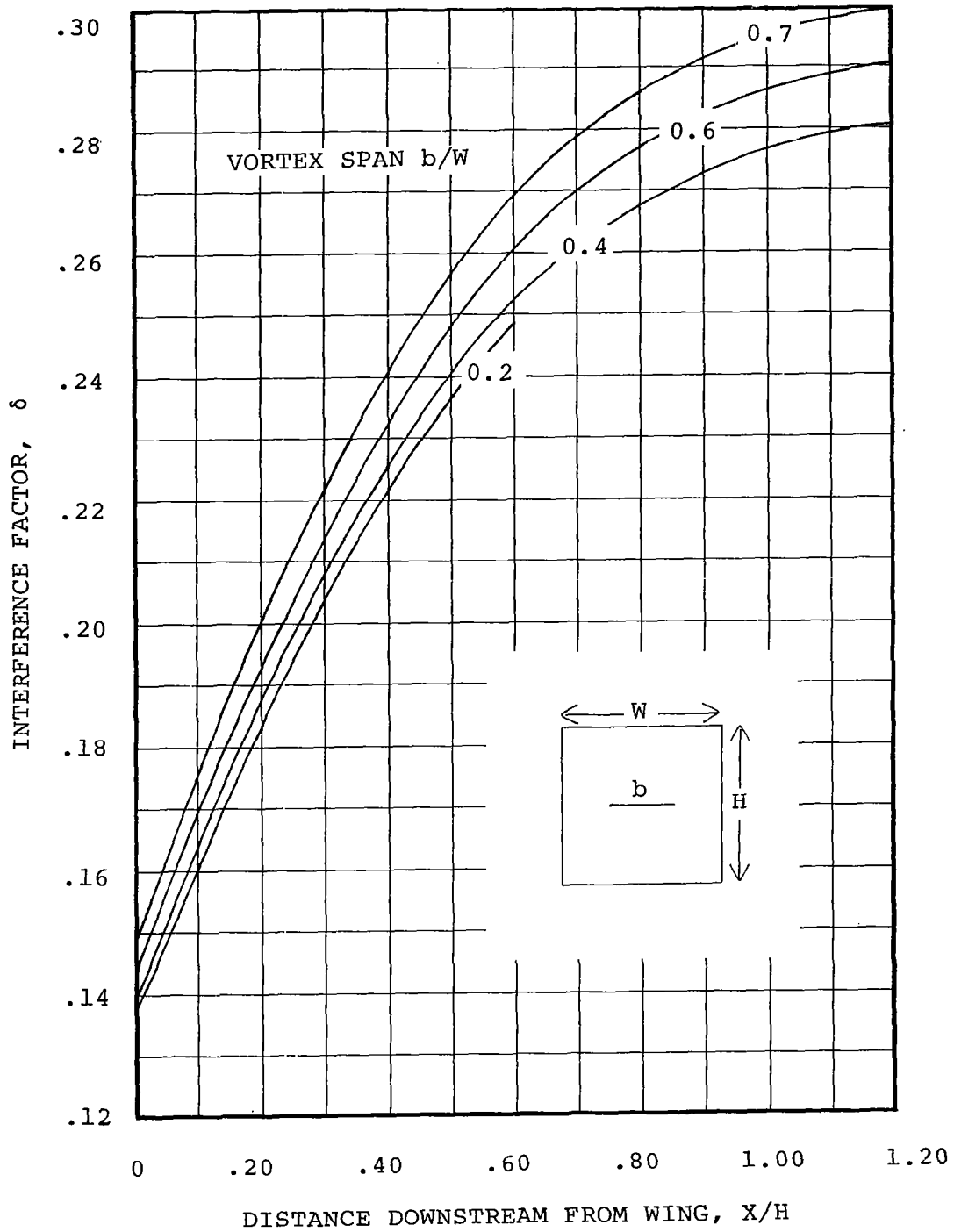


FIGURE 6

WALL INTERFERENCE FACTORS
FOR A 3:5 RECTANGULAR WIND TUNNEL

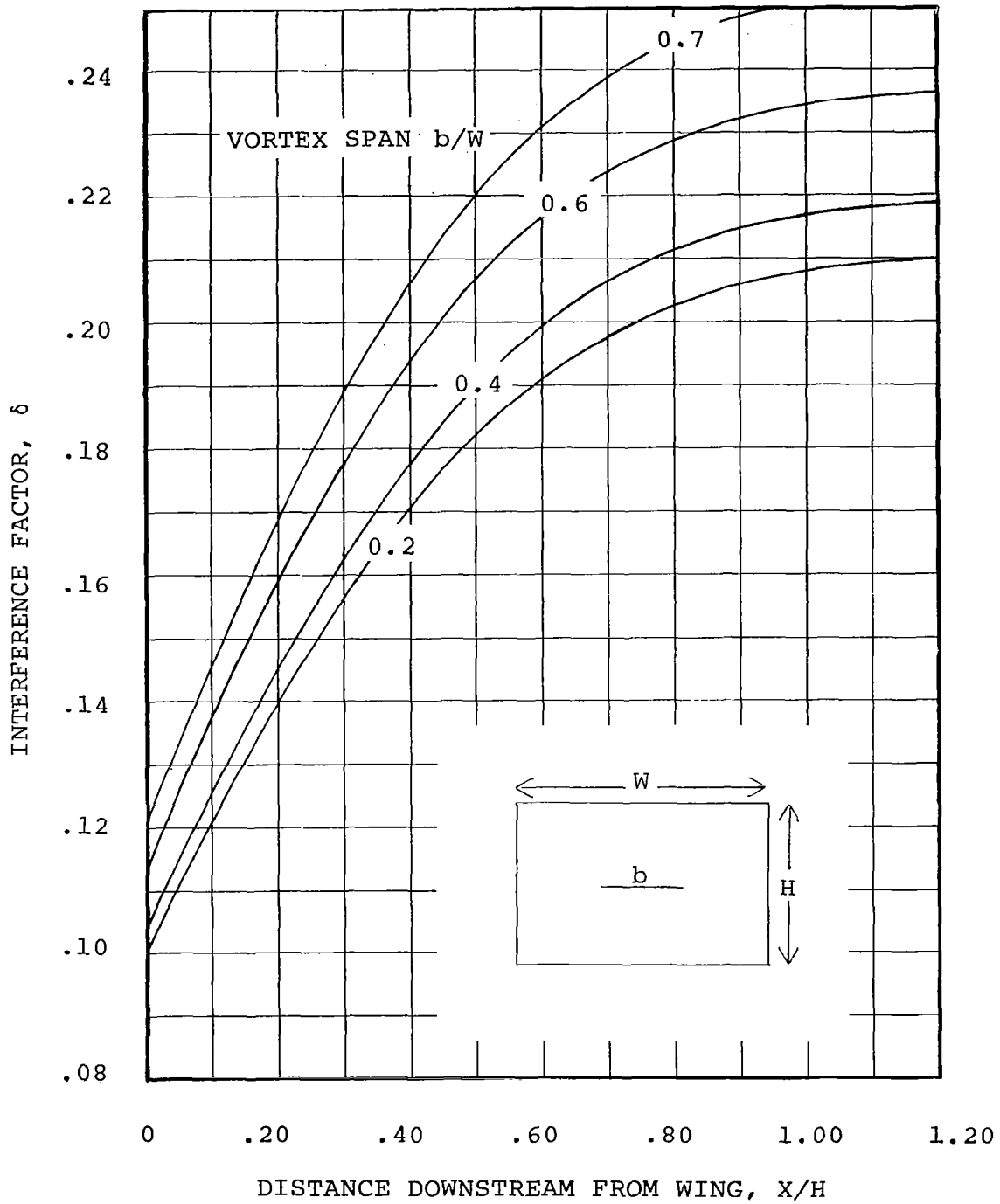


FIGURE 7

EFFECT OF WING SPAN ON AVERAGE INTERFERENCE FACTOR
AND THE CENTERLINE INTERFERENCE FACTOR AT THE WING

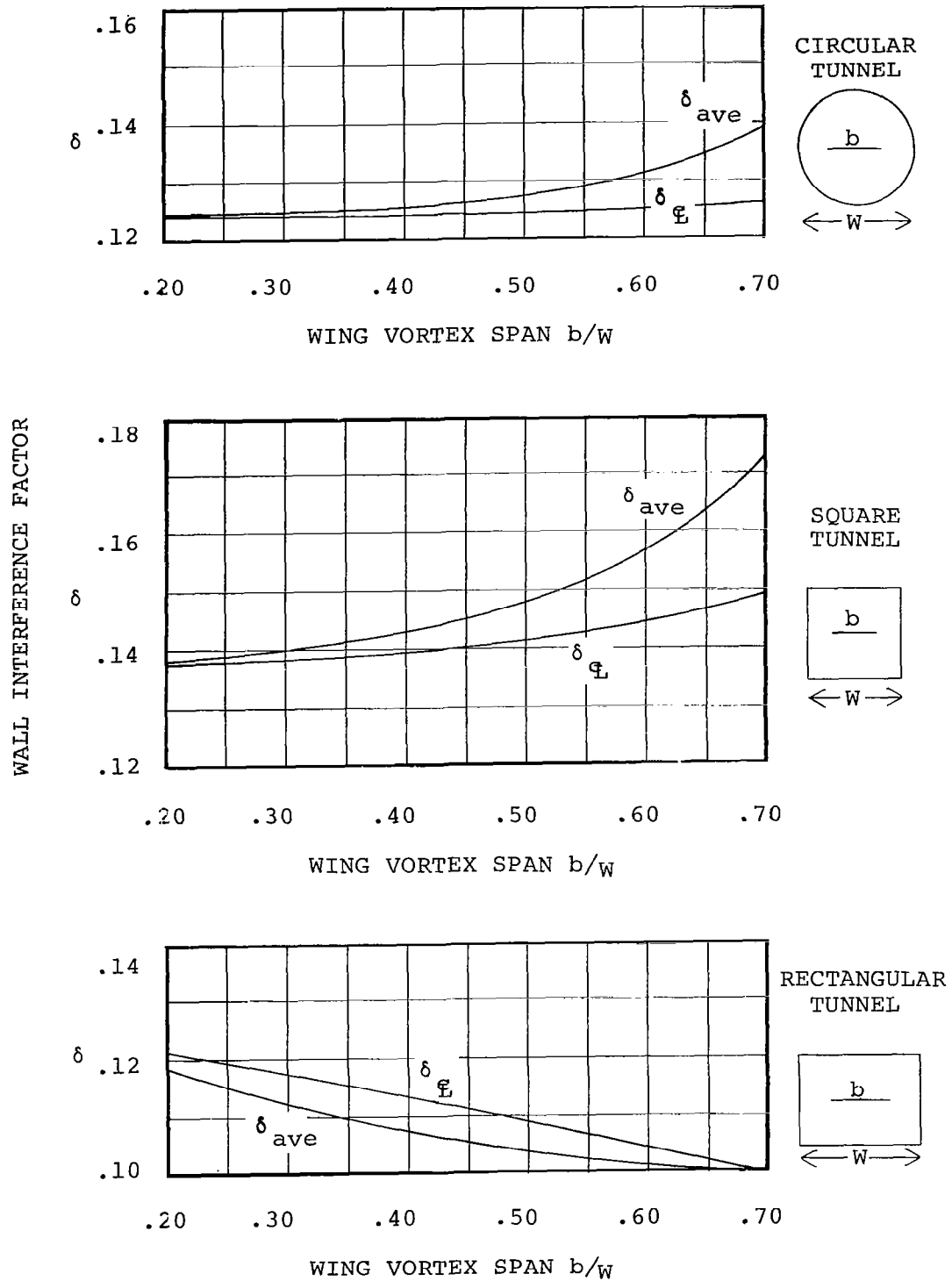


FIGURE 8

COMPARISON OF INTERFERENCE FACTORS
WITH CLASSICAL VALUES FOR A SQUARE TUNNEL

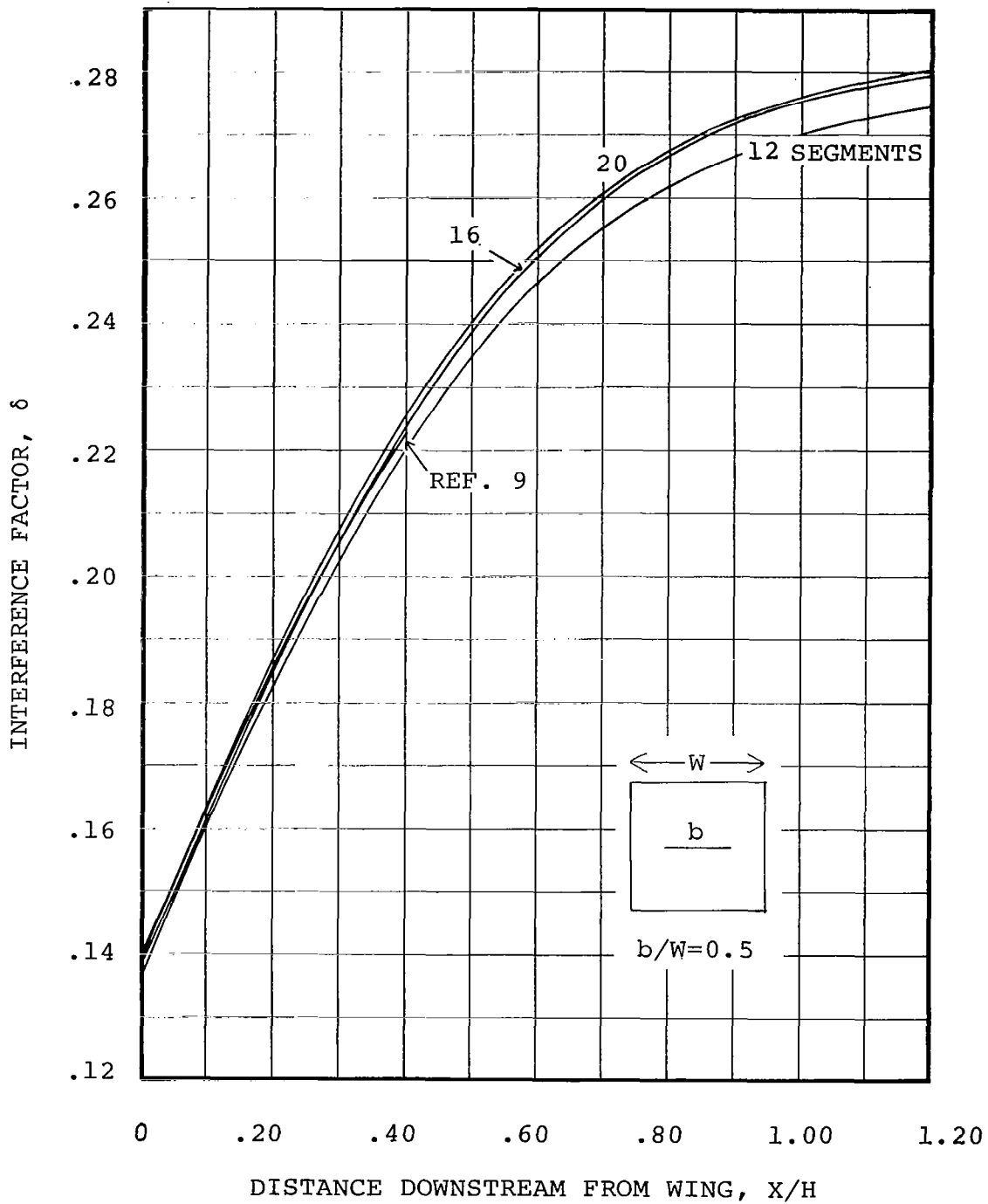


FIGURE 9

COMPARISON OF INTERFERENCE FACTORS
WITH CLASSICAL VALUES FOR A CIRCULAR TUNNEL

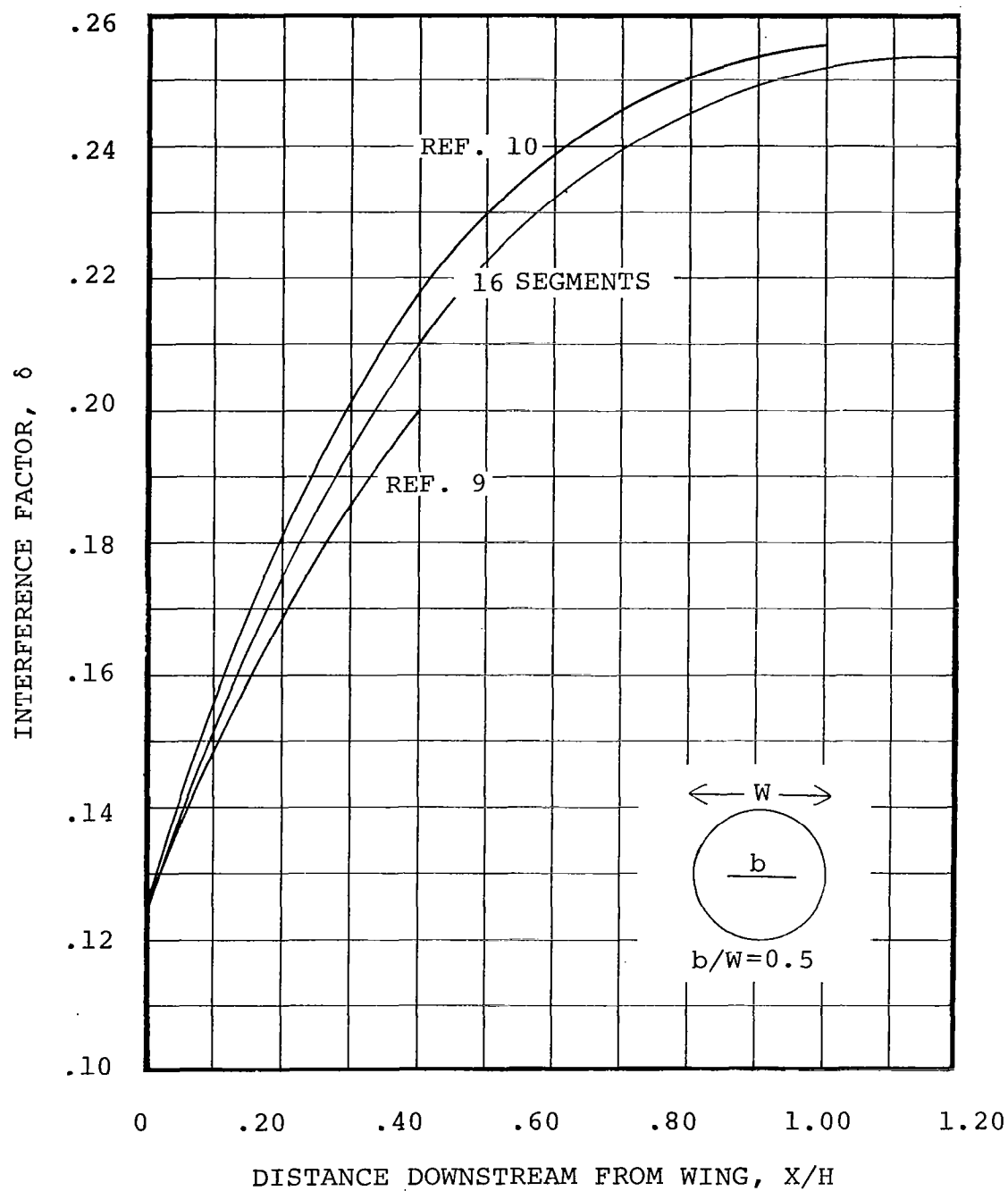


FIGURE 10

EFFECT OF TUNNEL LENGTH ON INTERFERENCE FACTORS
FOR A CIRCULAR TUNNEL

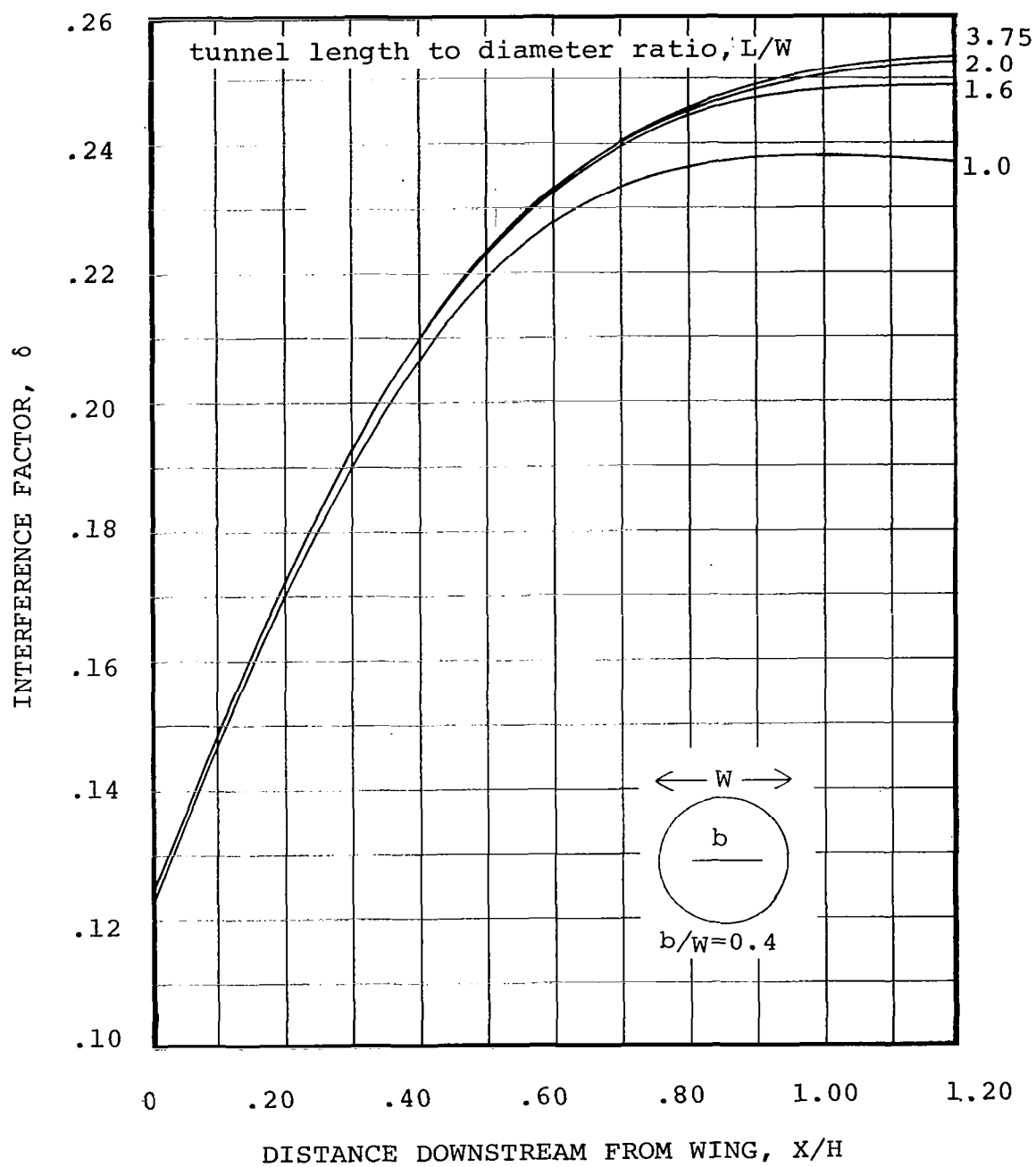


FIGURE 11

EFFECT OF TUNNEL LENGTH ON WALL VORTICITY DISTRIBUTION
FOR A CIRCULAR TUNNEL

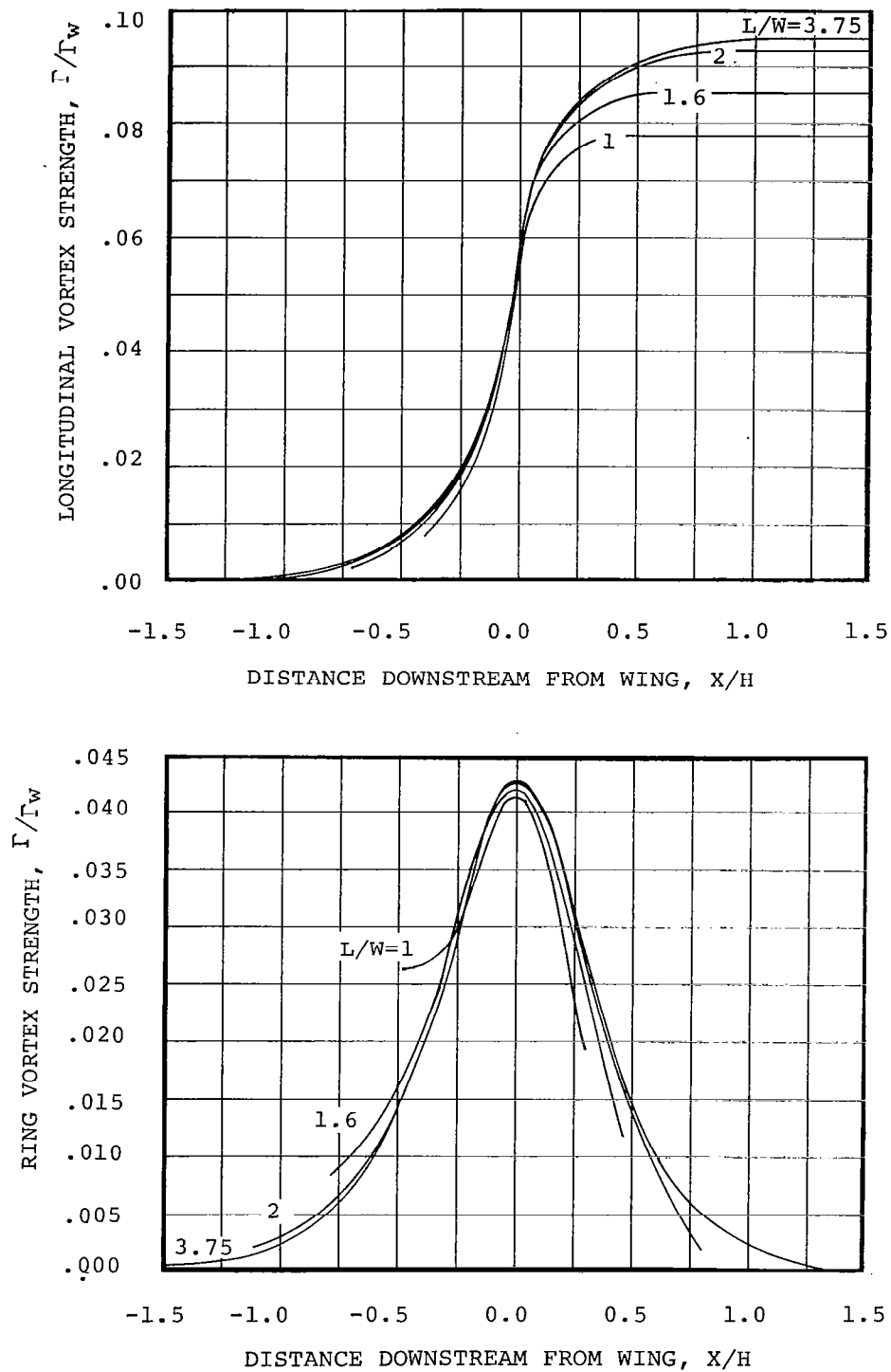


FIGURE 12

"The aeronautical and space activities of the United States shall be conducted so as to contribute . . . to the expansion of human knowledge of phenomena in the atmosphere and space. The Administration shall provide for the widest practicable and appropriate dissemination of information concerning its activities and the results thereof."

—NATIONAL AERONAUTICS AND SPACE ACT OF 1958

NASA SCIENTIFIC AND TECHNICAL PUBLICATIONS

TECHNICAL REPORTS: Scientific and technical information considered important, complete, and a lasting contribution to existing knowledge.

TECHNICAL NOTES: Information less broad in scope but nevertheless of importance as a contribution to existing knowledge.

TECHNICAL MEMORANDUMS: Information receiving limited distribution because of preliminary data, security classification, or other reasons.

CONTRACTOR REPORTS: Scientific and technical information generated under a NASA contract or grant and considered an important contribution to existing knowledge.

TECHNICAL TRANSLATIONS: Information published in a foreign language considered to merit NASA distribution in English.

SPECIAL PUBLICATIONS: Information derived from or of value to NASA activities. Publications include conference proceedings, monographs, data compilations, handbooks, sourcebooks, and special bibliographies.

TECHNOLOGY UTILIZATION PUBLICATIONS: Information on technology used by NASA that may be of particular interest in commercial and other non-aerospace applications. Publications include Tech Briefs, Technology Utilization Reports and Notes, and Technology Surveys.

Details on the availability of these publications may be obtained from:

SCIENTIFIC AND TECHNICAL INFORMATION DIVISION
NATIONAL AERONAUTICS AND SPACE ADMINISTRATION

Washington, D.C. 20546